

PyDaddy: A Python package for discovering stochastic dynamical equations from time series data

Arshed Nabeel,^{1,*} Ashwin Karichannavar,^{1,†} Shuaib Palathingal,¹
Jitesh Jhawar,^{2,3} Danny Raj M.,⁴ and Vishwesha Guttal^{1,‡}

¹Center for Ecological Sciences,

Indian Institute of Science, Bengaluru, India

²University of Konstanz, Konstanz, Germany

³Max Planck Institute of Animal Behaviour, Konstanz, Germany

⁴Department of Chemical Engineering,

Indian Institute of Science, Bengaluru, India

(Dated: November 4, 2022)

1. Ecological dynamics, ranging from individual behaviours to ecosystem dynamics, are inherently stochastic in nature. *Stochastic differential equations* (SDEs) are an important modelling framework to model dynamics with intrinsic randomness. Here, we focus on the inverse question: If one has empirically measured time series data from some system of interest, is it possible to discover the SDE model that best describes the data?

2. We present PyDaddy (Python library for **D**ata **D**riven **D**ynamics), a toolbox to construct and analyse interpretable SDE models based on time series data. We combine traditional approaches for data-driven SDE reconstruction with an *equation learning* approach, to derive symbolic equations governing the stochastic dynamics. The toolkit is presented as an open-source *Python* library, and consists of tools to construct, visualise, and analyse SDEs.

3. PyDaddy takes a time series as an input, and produces an interpretable, analytical expression for the underlying SDE. The package includes functionalities for visual examination of the stochastic structure of the data, guided extraction of an analytical expression for the SDE, and diagnosis and debugging of the underlying assumptions and the extracted model. Using simulated time series datasets, exhibiting a wide range of dynamics, we show that PyDaddy is able to correctly identify underlying SDE models. We demonstrate the applicability of the toolkit to real-world data using a previously published movement data of a fish school. The model discovered by PyDaddy is consistent with the previous study.

4. PyDaddy is an easy-to-use, open source package to discover SDEs that govern the dynamics of time series data. The package, together with the documentation and tutorial notebooks (which can be executed online even without installation) are available at: <https://pydaddy.readthedocs.io/>

Keywords: Data Driven Model Discovery, Langevin Dynamics, Self-organisation, Collective motion, Mesoscale dynamics, Data Driven Dynamical Systems, Scientific Machine Learning, Noise induced order

I. INTRODUCTION

A central approach to modelling complex dynamical systems, across fields including ecology, is via differential equations [1, 2]. Depending on the importance of space and stochasticity in the system, these equations can be ordinary, stochastic, or partial differential equations. Even when we begin with a simple set of rules or interactions at a fine, local scale, one can derive coarse-grained dynamical descriptions in the form of differential equations. For example, in the context of ecological populations, the local rules could be based on birth or death processes [3], movement and interactions between organisms [4–7], interactions of organisms with the environment [8, 9], etc. These local interactions scale to shape the dynamics at higher levels such as groups, populations or even ecosystems [7, 9–12]. While such

dynamical system based approaches are powerful and have provided key biological insights, integrating empirical data with such models continues to remain a challenge.

We are in the era of big data, where high-resolution data capturing the dynamics of biological systems is increasingly available [13, 14]. Examples span across scales of biological organisation, from individual (cells or animals) movement trajectories [14] and group properties [5, 15, 16] to population sizes [17, 18], fitness of populations [19] and ecosystem states [20–22]. Importantly, data maybe available with high temporal resolutions, sometimes even across space, thus opening avenues for better integration between models and data.

To capture the dynamics of real-world systems accurately, one has to treat state variables as stochastic rather than only accounting for the average properties [8]. Not only is randomness intrinsic to biological systems, it may also produce counter-intuitive effects that are absent in purely deterministic systems [11, 23]. A suitable framework for analysing stochastic dynamics is *stochastic differential equations* (SDE), which allows us to cap-

* Corresponding author; arshed@iisc.ac.in

† Equal contribution.

‡ Co-corresponding author; guttal@iisc.ac.in

ture both the deterministic and stochastic factors driving the dynamics. In the context of integrating theory and data, we focus on the following central question: can we construct stochastic dynamical models starting from observed time series datasets?

Indeed, the answer is in the affirmative. Traditional approaches to stochastic calculus, based on estimating so-called *jump moments*, allow us to infer stochastic differential equations from time series data [24–28]. More recently, techniques based on neural networks have also been developed for SDE discovery [29, 30]. In the context of deterministic models, recently developed *equation learning* techniques allow us to discover simple, interpretable differential equation models from time series data [31, 32]. Combining equation learning with the traditional methods of jump moments is powerful, since it allows us to extract parsimonious and interpretable SDE models directly from data [33–35]. However, these techniques are scattered across physics and engineering literature and lack diagnostic tools. Thus, there is a need for an end-to-end, user-friendly tool that takes in time series data, applies these methods, outputs an SDE model and provides diagnostic tools together with visualisations.

To address this gap, we introduce **PyDaddy** (Python library for Data Driven Dynamics), a comprehensive and easy-to-use Python package for discovering stochastic differential equations from empirical data. The package takes a time series of a state variable (scalar or vector) as the input, and outputs an interpretable SDE model. The package also implements a variety of visualisation and diagnostic utilities. We illustrate the workflow of the PyDaddy with the help of a real dataset from the collective animal motion literature [15]. We also provide a detailed documentation along with ready-to-use Python tutorial notebooks with a number of example datasets, to make the package easy to use (see Data and Code availability section). We highlight that the tutorial notebooks can be used without installation via Google Colab: <https://pydaddy.readthedocs.io/en/latest/tutorials.html>.

II. DISCOVERING SDE MODELS FROM TIME SERIES DATA

A. Method: Combining jump moments and equation learning

Consider a time series of some observed variable, such as population size or a measure of group’s movement, denoted by x , captured at a high temporal resolution. We wish to discover an equation governing the dynamics of x , capturing both the deterministic and stochastic aspects. This can be done using a stochastic differential equation of the form,

$$\dot{x} = f(x) + g(x)\eta(t) \quad (1)$$

(interpreted in the *Itô sense*) that describes the temporal dynamics of x . Here, f and g are functions of x , and $\eta(t)$ is Gaussian white-noise [36].

Eq. 1 describes how the rate of change of x depends on the instantaneous value of x . The average rate of change of x over time is governed by f , called the deterministic or *drift* function. The fluctuation around the average value is governed by g^2 , called the stochastic or *diffusion* function. When g is a constant (i.e. independent of x), the strength of the noise is the same for all values of x , and is called *additive* or *state-independent* noise. When g depends on x , the strength of the noise depends on the instantaneous value of x , and is called *multiplicative* or *state-dependent* noise [23].

Our goal is to discover the drift (f) and diffusion functions (g^2) from the observed time series data. Specifically, we aim to find simple, interpretable analytical expressions that describe f and g^2 , not just the qualitative shape. Our approach to this problem involves two steps (see SI Section S1 for the full mathematical details of the procedure):

1. First, we extract the drift and diffusion components from the given time series data, using the so-called *jump moments* or the *Kramer-Moyal coefficients* [26].
2. Next, we use a technique based on sparse regression, sometimes referred to as *equation learning*, to find interpretable analytical expressions of the extracted drift and diffusion functions [31, 33].

Conventional SDE estimation approaches usually stop with the first step. The drift and diffusion functions are estimated as binned averages, based on user input values of bin sizes and sampling time; although studies provide some rules of thumb for selecting these parameter values, the results can dramatically vary if incorrect values are given [27]. By combining the conventional approach with sparse-regression-based equation discovery techniques, our approach in PyDaddy precludes the need of arbitrary parameter choices. In addition, the accuracy of the estimates is also considerably improved, even when the available time series is short (see SI Section S3).

Modelling a given time series using an SDE is contingent on several assumptions: for instance, the noise term η is assumed to be uncorrelated Gaussian noise. Therefore, the data-driven SDE discovery pipeline is incomplete without sufficient diagnostic tests to make sure that the assumptions are reasonably satisfied.

The following assumptions need to hold for the estimation to be accurate [26, 37]:

- The residuals, defined as $r(t) = \dot{x}(t) - F(x(t))$, should be normally distributed around 0. For vector time series, the residuals should also be isotropic, i.e. the x_i - and x_j -components of the residuals should be uncorrelated for $i \neq j$.

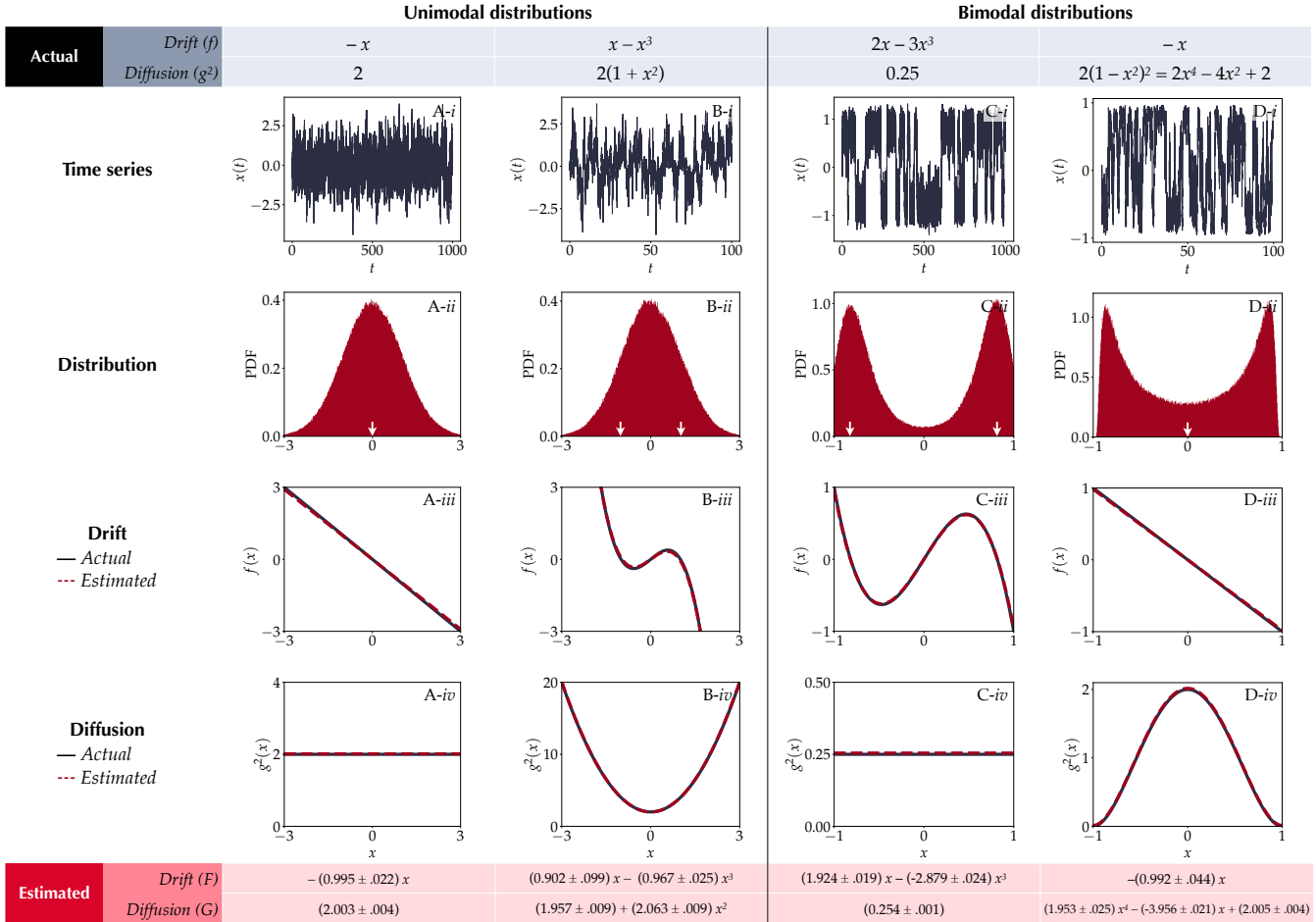


FIG. 1. **Sparse regression on the extracted instantaneous jump moments reliably reconstructs governing equations from simulated data, for a wide range of dynamics.** The mathematical expressions for the actual and estimated drift and diffusion functions are shown in the tables on the top (grey shaded) and bottom (red shaded), respectively. Row i shows a sample of the time series $x(t)$ of the models Eqs 2-5, respectively, across four columns (A-D), while row ii shows the corresponding histograms of $x(t)$. The arrows in histograms in row ii mark the deterministic stable equilibria of the respective systems. Notice that the histograms in (A) and (B) are identical, despite the underlying SDEs being very different. Similarly, the histograms in (C) and (D) are similar. (A) A simple Ornstein-Uhlenbeck process (Eq. 2), with a linear drift and constant diffusion, giving rise to a unimodal probability distribution of $x(t)$ that coincides with the deterministic stable equilibrium. (B) A system with a cubic drift and a quadratic diffusion function (Eq. 3), also giving rise to a unimodal probability distribution of $x(t)$. The deterministic part of this system has two stable equilibria (two arrows in B-ii). However, due to the effect of stochasticity, we observe only one mode of the time series which coincides with the unstable deterministic equilibrium. (C) A system with cubic drift and constant diffusion (Eq. 4) giving rise to a bimodal probability distribution. The bimodality here is explained entirely by deterministic equilibria, with noise facilitating transitions between them. (D) A system with a linear drift and a quadratic diffusion (Eq. 5), giving rise to a bimodal probability distribution. The deterministic part of the system has only one stable equilibrium at 0. Hence, the bimodality here is driven by stochasticity. Rows iii and iv compare the ground-truth (black) drift and diffusion functions with the estimated ones. The functions estimated using sparse regression are shown as dark red dashed lines. In all cases, the proposed method accurately recovers the drift and diffusion functions.

- The residuals should be uncorrelated across time.
- *Pawula's Theorem:* Similar to the drift and diffusion components, one can also estimate higher moments from the data. Pawula's theorem states that, for a drift-diffusion SDE, the third and higher moments should be zero [36]. In practical scenarios, where we have a finite-length time series sampled at a finite sampling time, the estimated higher

moments will not go to zero in general. In this case, alternative to Pawula theorem would be that $K_4(x) \approx 3 \cdot K_2(x)^2$, where K_2 and K_4 are the second and forth Kramers-Moyal moments respectively. [26, 38]

In addition to this, there is also the issue of *model identifiability*: how can we be confident that the model we identify is the only (or at the very least, the 'best') model

that describes the observed data? One way to address this is to look at the self-consistency of the estimated model [27]. Suppose we estimate an SDE model using our approach. If we generate a simulated time series using this estimated model, with identical length and sampling interval as the original time series, then:

- The simulated time series should have the same statistics—namely, histogram and autocorrelation—as the original time series.
- If we subsequently estimate a model from the simulated time series, this model should match the originally estimated model.

B. Demonstration of the method from synthetic datasets

To demonstrate the estimation performance of the proposed method, we evaluated the method on several simulated systems where the ground-truth governing dynamics are known. We generated synthetic data from known SDEs, using several different choices of f and g . We then used our approach to estimate $f(x)$ and $g(x)$ from the simulated time series.

We consider the following two SDEs:

$$\dot{x} = -x + \sqrt{2} \cdot \eta(t) \quad (2)$$

$$\dot{x} = x - x^3 + 2(\sqrt{1+x^2}) \cdot \eta(t) \quad (3)$$

Although Eq. 2 and 3 are quite different, the time series generated with these equations as well as their histograms are very similar (Fig. 1 (A-i, A-ii, B-i, B-ii)): in fact, the steady-state distribution of $x(t)$ will be identical for Eq. 2 and 3. Specifically, Eq. 2 has a single deterministic stable state at $x^* = 0$, which is reflected in the histogram as well (Fig. 1 (A-ii)). The additive noise simply spreads the dynamics around the deterministic equilibrium. On the other hand, the deterministic stable equilibria for Eq 3 are at ± 1 but the mode of the histogram is at 0 (Fig. 1 (B-ii)). In this case, the multiplicative noise-term completely alters the stability landscape, annihilating the deterministic stable states and creating a new noise-induced mode at $x = 0$.

Similarly, consider another pair of SDEs:

$$\dot{x} = 2x - 3x^3 + \frac{1}{2} \cdot \eta(t) \quad (4)$$

$$\dot{x} = -x + \sqrt{2}(1-x^2) \cdot \eta(t) \quad (5)$$

Eq. 4 has two deterministic stable equilibria at $\pm \sqrt{2/3}$, and the dynamics is spread around these equilibria by the additive noise (Fig. 1 (C-ii)). On the other hand, Eq. 5 has only one stable equilibrium at $x = 0$; yet, due to the effect of the noise term, the system exhibits the two modes in the histogram away from the deterministic equilibrium (Fig. 1 (D-ii)).

Distinguishing between 2 and 3 (similarly 4 and 5) from either the time series data or steady state distributions is challenging. Nevertheless, our approach is able to distinguish these systems and extract the correct governing SDE in each case (Fig. 1 rows iii and iv). We are also able to recover the analytical expressions for the drift and diffusion functions almost exactly.

III. THE PYDADDY PACKAGE

We implement our technique for data-driven SDE discovery as a Python package, **PyDaddy** (Python library for **D**ata **D**riven **D**ynamics). In addition to the SDE discovery functionality, based on combining sparse regression with the computation of Kramer-Moyal coefficients (see SI Section 1), PyDaddy offers many diagnostic and visualisation features that lets the user explore and evaluate the results. PyDaddy takes either a scalar or 2-dimensional vector data as the input, where the visualisations and diagnostics are most effective. From a given uniformly sampled 1-D or 2-D time series, PyDaddy can compute, visualise, and fit drift and diffusion functions. PyDaddy supports time series with missing data. Diagnostic tools are provided to verify whether the assumptions necessary for modelling the time series as an SDE are met. Finally, PyDaddy can export data into a DataFrame or a CSV file. Fig. 2 shows an overview of the package and its various functionalities.

For ease of use, we make the package and the associated tutorial notebooks accessible online, even without installation, via Google Colab: <https://pydaddy.readthedocs.io/en/latest/usage.html#pydaddy-on-google-colab>.

The package can also be installed on a local machine using PIP or Conda:

```
pip install pydaddy
```

or

```
conda install pydaddy -c tee-lab
```

PyDaddy features a single-command operation mode, which allows the user to run a dataset through PyDaddy and generate a comprehensive HTML report. This can be done using the command:

```
pydaddy <dataset-file-name>
```

The report contains interactive figures of the estimated drift and diffusion functions (with default parameters and automatic threshold tuning—see below) and diagnostic results about noise statistics and model self consistency.

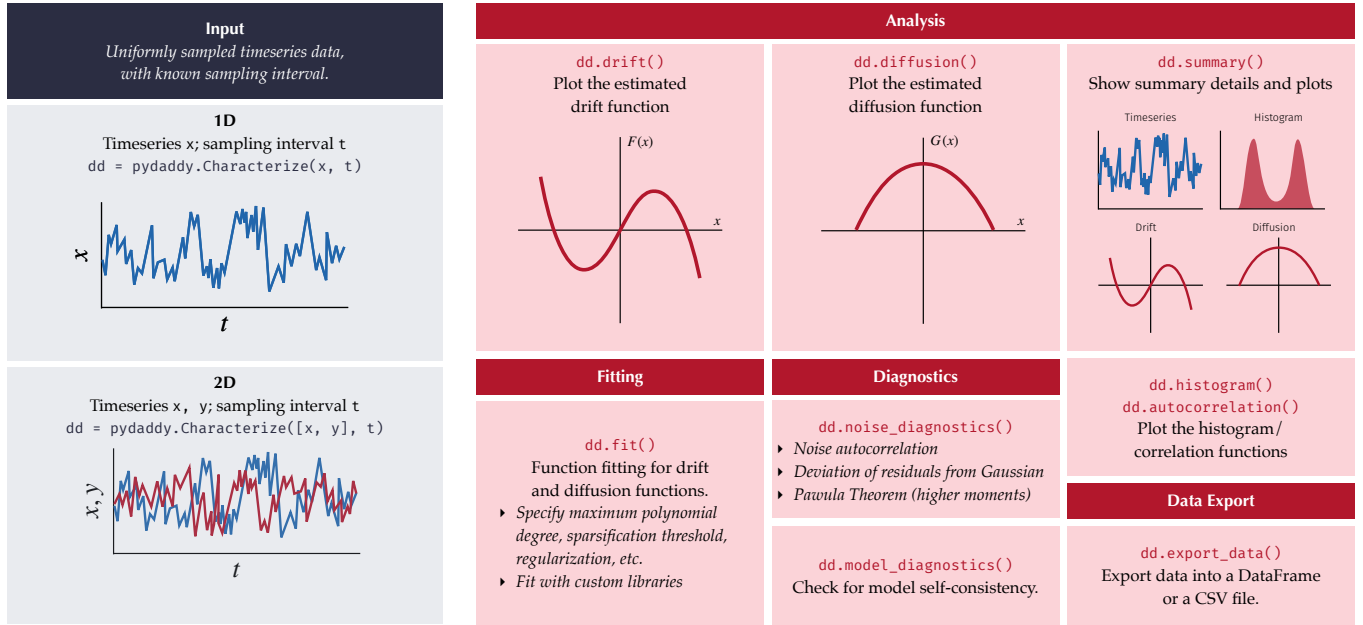


FIG. 2. Overall schematics of the PyDaddy package. PyDaddy takes as input uniformly sampled 1D or 2D time series, and computes the drift and diffusion components from the time series. Several functions are provided to visualise data as time series or histograms, fit drift and diffusion functions, diagnose whether underlying assumptions for drift-diffusion estimation are met, and to export data.

PyDaddy also has a comprehensive Python API for advanced usage; which allows the user to individually generate various plots, perform diagnostics, or fine-tune the function fitting procedure.

A. SDE estimation workflow using a real dataset

We now demonstrate the PyDaddy estimation workflow, using a previously published dataset of fish schooling [15]. Briefly, the dataset contains the time series of the group polarisation vector, $\mathbf{m} = (M_x, M_y)$ (2-dimensional), for a group of 15 fish (*Etroplus suratensis*). The time series is available at a uniform interval of 0.12 second, with many missing data points. If the school of fish is highly ordered, with nearly all fish moving in the same direction, the magnitude of the polarisation vector, $|\mathbf{m}|$, will be closer to 1. On the other hand, if the group is disordered, with fish moving in random directions, $|\mathbf{m}|$, will be close to 0.

Authors [15] extracted an SDE that governs the group polarisation \mathbf{m} , using the conventional approaches. Here, we will use this dataset with PyDaddy to derive an SDE for \mathbf{m} .

1. Summary figure and estimation of drift and diffusion

The estimation workflow starts by creating a PyDaddy object dd , initialised with a dataset.

```
dd = pydaddy.Characterize([x, y], t=0.12)
```

where x and y are Numpy arrays of the m_x and m_y time series respectively. A summary figure is generated with basic statistics of the time series such as the autocorrelation function and histograms of \mathbf{m} (Fig. 3). The summary figure also shows a preliminary estimate of the drift and diffusion functions, using binwise averaged conditional moments (see [15, 27] for more details on the binwise averaging method).

2. Fitting analytical expressions for drift and diffusion functions

The drift and diffusion plots above can be used to identify qualitative features of the dynamics, such as the nature and positions of the deterministic equilibrium points, nature of the state-dependent noise (i.e. diffusion), presence or absence of cross diffusion, etc. PyDaddy can go a step beyond and fit actual analytical expressions for the drift and diffusion functions. This can be done using the `fit()` function of the `dd` object.

As mentioned in Section II A, fitting is done using sparse regression. By default, PyDaddy fits polynomial functions, but other function families can also be fit using custom libraries. A *sparsification threshold*, which governs the number of terms in the fit (see SI Section S1B) can be either chosen automatically using cross-

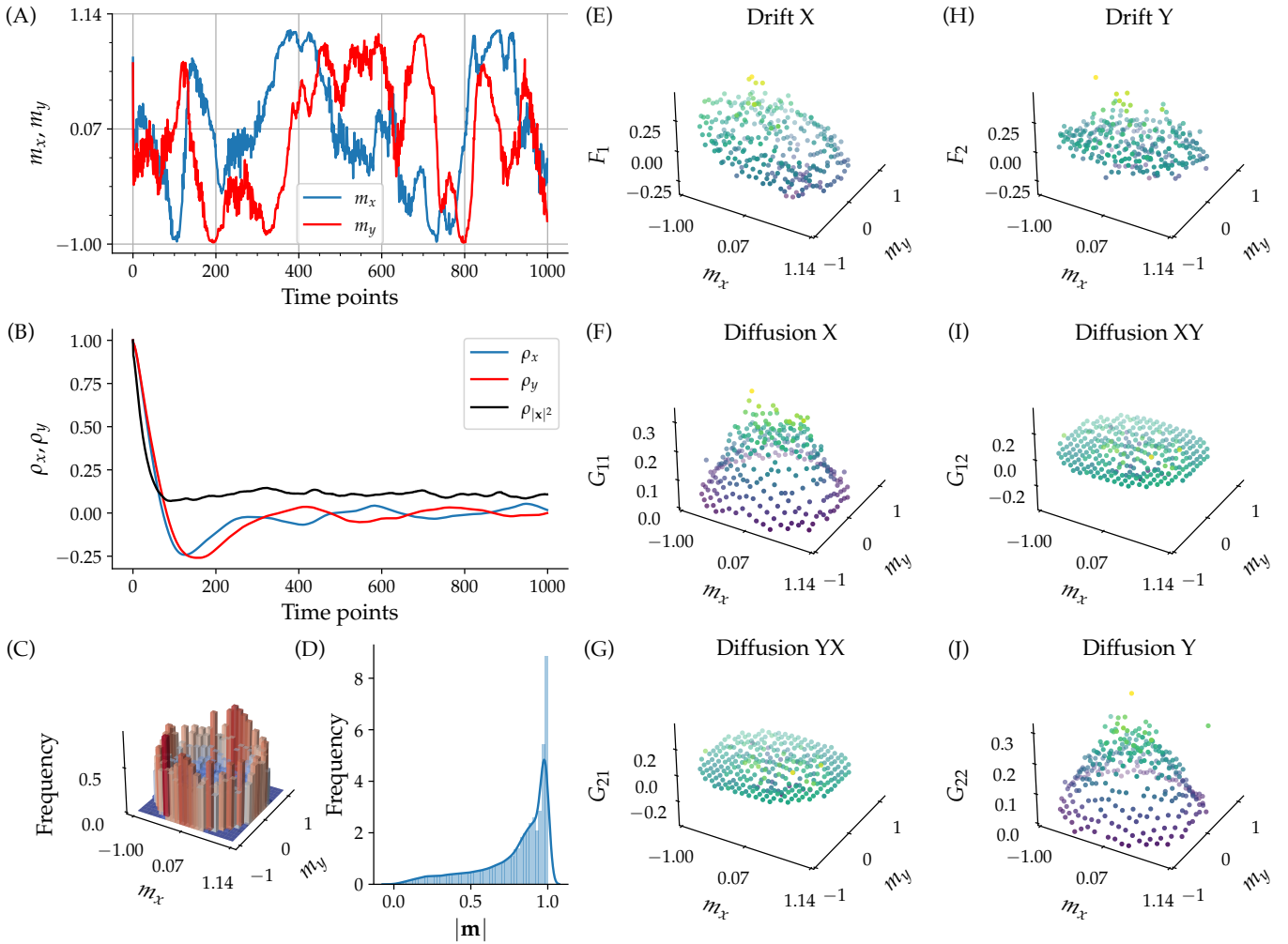


FIG. 3. The summary plot generated by PyDaddy when applied to schooling fish data from the reference [15]. (A) Input time series (fish group polarisation), a vector time series denoted by $\mathbf{m} = (M_x, M_y)$. One time step corresponds to 0.12 s. (B) Autocorrelation functions of the time series, showing that the autocorrelation decays with time. (C, D) Frequency histograms of \mathbf{m} and $|\mathbf{m}|$, depicting that the most likely state of the fish group is schooling (i.e. highly polarised). (E, H) Preliminary estimates of drift functions. (F, G, I, J) Preliminary estimates of diffusion functions. The drift and diffusion functions shown here are bin-wise averages of the jump moments (bin-wise averaging is done only for the visualisation).

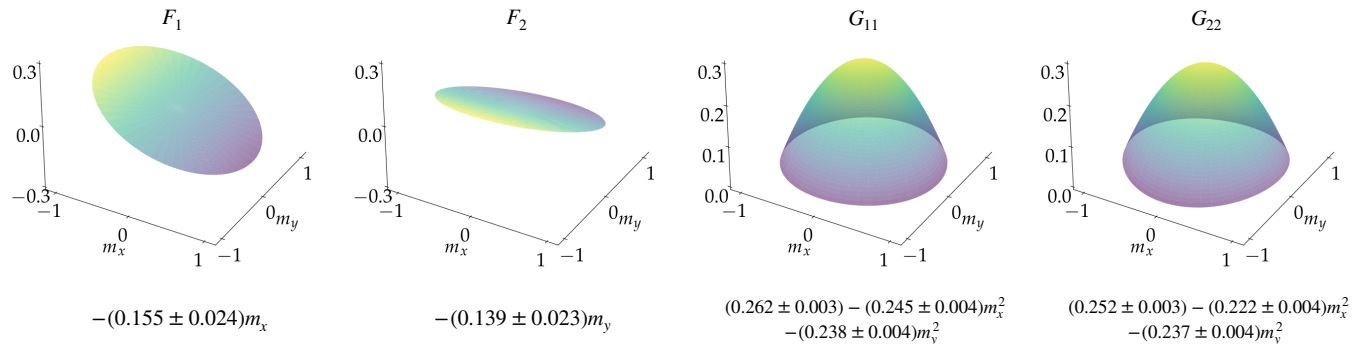


FIG. 4. Interpretable drift and diffusion functions estimated by PyDaddy using the sparse regression method. The estimated interpretable functions returned by PyDaddy are shown below each of the plots. F_1 and F_2 are the components of the drift function, and G_{11} and G_{22} are the components of the diffusion function. (The cross diffusion function $G_{12} = G_{21}$ was estimated to be identically 0, and is not shown.)

validation (see SI Section S1C), or be set manually.

For example,

```
dd.fit('F1', order=3, tune=True,
plot=True)
```

fits a degree-3 polynomial (`order=3`) with sparsification threshold chosen automatically (`tune=True`). The first argument names the function to be fitted: `F1` and `F2` correspond to the two components of the drift; `G11` and `G22` correspond to diffusion, and `G12` and `G21` correspond to cross diffusion. The `plot=True` argument tells the function to produce a cross-validation error plot for a range of thresholds (see SI Fig. S1). The ideal threshold should strike a balance between the error and number of terms in this plot. PyDaddy chooses as high as a threshold as possible without increasing the cross-validation error too much (see SI Section S1C for details).

The threshold can also be manually set by the user. For example,

```
dd.fit('F1', order=3, threshold=0.1)
```

produces a polynomial with degree up to 3, with only terms with coefficients 0.1 or higher.

Fig. 4 shows the drift and diffusion functions estimated by PyDaddy for the example time series. In line with previous results [15], we find a linear drift and a quadratic diffusion, suggesting that the group polarisation is noise-induced. The cross-diffusion terms (not shown) were negligible and were fit by the zero polynomial.

In the drift and diffusion functions in Fig. 4, coefficients with overlapping error-bars can be combined (by replacing them with their averages), to get the following vector SDE:

$$\dot{\mathbf{m}} = -0.147\mathbf{m} + \sqrt{0.021 + 0.236(1 - |\mathbf{m}|^2)} \cdot \boldsymbol{\eta}(t) \quad (6)$$

where we used \mathbf{m} to represent the group polarisation in the estimated equation. This equation is consistent with the result of [15].

We emphasize an important point here: although PyDaddy provides functionality for automatic model selection, model selection works best when coupled with some human input based on theory and understanding of the system. In particular, we suggest that the maximum order of the polynomial, or more generally the library of function to fit, needs to be specified based on visual inspection of the drift/diffusion plots in conjunction with a theoretical understanding of the system. The PyDaddy documentation [39] contains an extended discussion about this aspect.

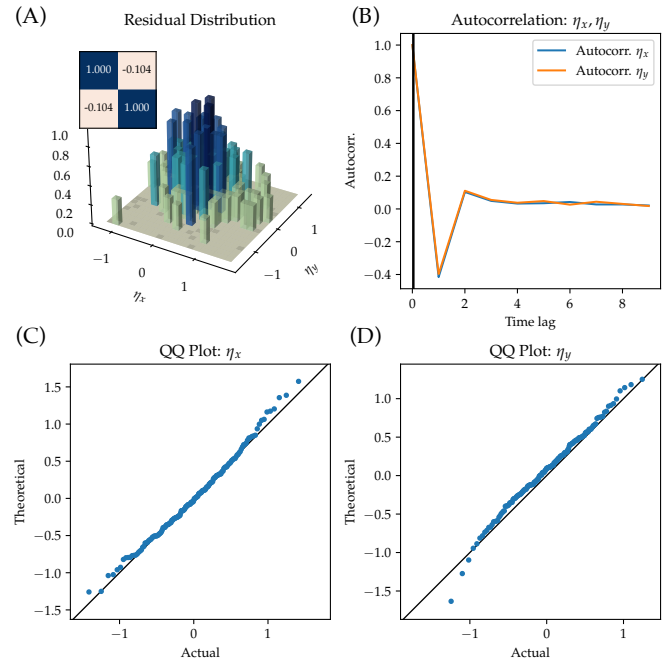


FIG. 5. **Noise diagnostics figure generated by PyDaddy.** (A) Distribution of the residuals, which resembles a bivariate Gaussian with zero mean. The inset matrix shows correlation matrix of the x and y components of the noise. This should be close to the identity matrix. (B) Autocorrelation functions of the residuals, with the black line marking the autocorrelation time and is close to zero, as desired. (C, D) QQ-plots of the marginal distributions, which nearly falls on a line of slope 1, again as desired by the assumptions of the SDE model.

3. Diagnostics

It is also essential to ensure that the assumptions involved in modelling the time series as an SDE (SI Section S1E) are not violated. PyDaddy provides diagnostic functions to verify that the assumptions are met. Diagnostic plots in PyDaddy can be generated using

```
dd.noise_diagnostics()
```

Fig. 5 shows the noise diagnostic plots produced by PyDaddy. The diagnostic plots show the distribution and autocorrelation of the residuals, and QQ-plots of the marginals of the residuals against a theoretical Gaussian distribution. These plots test for deviations of the residuals from an uncorrelated Gaussian distribution (see Section II A for details).

In addition, PyDaddy can also perform a model self-consistency check (Section S1E) using the following command:

```
dd.model_diagnostics()
```

This function uses the estimated SDE to generate a simulated time series, with the same length and sampling interval as the original dataset. It then estimates the drift and diffusion functions from the simulated time series, using the same order and threshold used in the original estimation. Finally, a summary figure is generated, comparing the histogram, drift and diffusion functions of the original dataset to the simulated dataset (SI Fig. S4). If the model is self-consistent, we expect a good match between the original and the simulated time series.

IV. DISCUSSION

Here, we have presented a Python package PyDaddy—an easy-to-use tool for data-driven discovery of dynamics of complex systems. Specifically, PyDaddy seeks to find a data-driven stochastic differential equation that captures the dynamics of the observed state variable. We combined the traditional approaches of drift and diffusion estimation using jump moments, with techniques based on sparse regression to recover SDE models from time series data. The use of sparse regression helped us eliminate certain arbitrary choices of parameters (such as bin-size and subsampling time) used in previous methods [27, 28]. Equally importantly, we provide visual and diagnostic tools to test the assumptions associated with data-derived functions, sparse fits, as well as the noise.

We demonstrated the method with a time series data of schooling fish. However, it is readily applicable to any ecological system, or more generally any dynamical system, where sufficiently highly resolved and long data are available. This raises the obvious question: how finely resolved and how long a time series is necessary? As demonstrated in previous studies [27], the time series must be at around an order of magnitude (or more) finely resolved than the autocorrelation time of the state variable. When the time resolution is comparable or more than the autocorrelation time, the dynamics of the system can't be captured; for such coarse time series, the estimated drift and diffusion functions typically converge to a linear and upward-parabolic functions, independent of the actual dynamics [28]. While we are not aware of any studies that have looked at the *minimum length* required to estimate the drift and diffusion reliably, based on our own numerical simulations of models shown in this study, we speculate that the total length must be at least a few orders of magnitude times the length of the autocorrelation time.

We expect many challenges, and hence opportunities for future work, when applying these methods to complex ecological systems. First, despite the fact that we have automated various steps, there are still a few choices the user will make. These include the choice of the functions the user will chose to fit and the sparsity threshold, since a less sparse function (i.e. one with

more terms) will always explain the variation of data better. We suggest that one must choose the best fit functions using the '*principle of parsimony*', and be guided by theory when possible. We have already alluded to the importance of length of time series, and how it may impact on what we find as best-fit functions. Secondly, in the current framework of SDEs, the structure of noise is Gaussian and uncorrelated. This could be too simplistic since many ecosystems are affected by different types of perturbations and stochasticity; for example, a single large natural or human induced calamity is better modelled as a shot noise rather than a Gaussian white noise [40]. Noise in real systems may also be temporally correlated [41]. Finally, the key drivers of the system may show seasonality (e.g. rainfall, nutrient flow), thus violating the assumption of stationarity which is necessary for discovering SDEs from time series data. Modifying and adopting the package described here to account for realistic features presents interesting directions for future work.

In summary, as the era of big data looms over much of biological sciences including ecology, we hope that our presentation of a (relatively) easy to use package that helps us characterise the governing dynamical equations from the data will inspire usage of these relatively unknown methods in the field of ecology and more broadly, to other complex dynamical systems.

DATA AND CODE AVAILABILITY

The full code and documentation for the PyDaddy package is available at <https://github.com/tee-lab/PyDaddy> and <https://pydaddy.readthedocs.io> respectively.

We provide several tutorial notebooks to familiarise the user with the package:

- Getting started with PyDaddy
- Getting started with vector data
- Recovering SDEs from SDE-generated time series
- Advanced function fitting
- Exporting data
- Fitting non-polynomial functions

The tutorial notebooks can be accessed here: <https://pydaddy.readthedocs.io/en/latest/tutorials.html>

PyDaddy also comes with some sample datasets:

- Real world data of fish schooling (taken from Jhawar et. al. [15])
- Data generated from stochastic agent-based simulations, in 1-D and 2-D, based on [27].

ACKNOWLEDGEMENTS

We acknowledge support from Science and Engineering Research Board (VG), CEFIPRA (VG), DST-FIST (VG), DST INSPIRE Faculty Award (DRM), Humboldt Postdoctoral Fellowship (JJ) and MoE PhD Fellowship (AN abd SP). We thank Ashrit Mangalwedhekar, Vivek Jadhav, Shikhara Bhat, Cassandre Aimon and Haris-

hankar Muppirala for comments on the package.

AUTHOR CONTRIBUTION

VG and DRM conceived the project. AN and AK developed the package, associated methods and performed analysis with inputs from all coauthors. AN, DRM and VG wrote the manuscript. All coauthors contributed to discussions and comments on the manuscript.

[1] S. H. Strogatz, *Nonlinear dynamics and chaos: with applications to physics, biology, chemistry, and engineering* (CRC press, 2018).

[2] N. J. Gotelli *et al.*, *A primer of ecology*, Vol. 494 (Sinauer Associates Sunderland, MA, 2008).

[3] A. J. McKane and T. J. Newman, Stochastic models in population biology and their deterministic analogs, *Physical Review E* **70**, 041902 (2004).

[4] H. Cheng, N. Yao, Z.-G. Huang, J. Park, Y. Do, and Y.-C. Lai, Mesoscopic interactions and species coexistence in evolutionary game dynamics of cyclic competitions, *Scientific Reports* **4**, 1 (2014).

[5] C. A. Yates, R. Erban, C. Escudero, I. D. Couzin, J. Buhl, I. G. Kevrekidis, P. K. Maini, and D. J. T. Sumpter, Inherent noise can facilitate coherence in collective swarm motion, *Proceedings of the National Academy of Sciences* **106**, 5464 (2009).

[6] M. A. Lewis, P. K. Maini, and S. V. Petrovskii, Dispersal, individual movement and spatial ecology, *Lecture Notes in Mathematics (Mathematics Bioscience Series)* **2071** (2013).

[7] J. Jhawar, R. G. Morris, and V. Guttal, Deriving Mesoscopic Models of Collective Behavior for Finite Populations, in *Handbook of Statistics*, Vol. 40 (Elsevier, 2019) pp. 551–594.

[8] A. J. Black and A. J. McKane, Stochastic formulation of ecological models and their applications, *Trends in ecology & evolution* **27**, 337 (2012).

[9] S. Majumder, A. Das, A. Kushal, S. Sankaran, and V. Guttal, Finite-size effects, demographic noise, and ecosystem dynamics, *The European Physical Journal Special Topics* **230**, 3389 (2021).

[10] M. Loreau, From populations to ecosystems, in *From Populations to Ecosystems* (Princeton University Press, 2010).

[11] R. Durrett and S. Levin, The importance of being discrete (and spatial), *Theoretical population biology* **46**, 363 (1994).

[12] T. Biancalani, L. Dyson, and A. J. McKane, Noise-induced bistable states and their mean switching time in foraging colonies, *Physical review letters* **112**, 038101 (2014).

[13] S. Leyk, A. E. Gaughan, S. B. Adamo, A. de Sherbinin, D. Balk, S. Freire, A. Rose, F. R. Stevens, B. Blankspoor, C. Frye, *et al.*, The spatial allocation of population: a review of large-scale gridded population data products and their fitness for use, *Earth System Science Data* **11**, 1385 (2019).

[14] R. Nathan, C. T. Monk, R. Arlinghaus, T. Adam, J. Alós, M. Assaf, H. Baktoft, C. E. Beardsworth, M. G. Bertram, A. I. Bijleveld, *et al.*, Big-data approaches lead to an increased understanding of the ecology of animal movement, *Science* **375**, eabg1780 (2022).

[15] J. Jhawar, R. G. Morris, U. Amith-Kumar, M. Danny Raj, T. Rogers, H. Rajendran, and V. Guttal, Noise-induced schooling of fish, *Nature Physics* **16**, 488 (2020).

[16] K. Tunstrøm, Y. Katz, C. C. Ioannou, C. Huepe, M. J. Lutz, and I. D. Couzin, Collective states, multistability and transitional behavior in schooling fish, *PLoS computational biology* **9**, e1002915 (2013).

[17] N. C. Stenseth, W. Falck, O. N. Bjørnstad, and C. J. Krebs, Population regulation in snowshoe hare and canadian lynx: asymmetric food web configurations between hare and lynx, *Proceedings of the National Academy of Sciences* **94**, 5147 (1997).

[18] O. N. Bjørnstad and B. T. Grenfell, Noisy clockwork: time series analysis of population fluctuations in animals, *Science* **293**, 638 (2001).

[19] R. E. Lenski, Experimental evolution and the dynamics of adaptation and genome evolution in microbial populations, *The ISME journal* **11**, 2181 (2017).

[20] S. R. Carpenter, B. M. Arani, P. C. Hanson, M. Scheffer, E. H. Stanley, and E. Van Nes, Stochastic dynamics of cyanobacteria in long-term high-frequency observations of a eutrophic lake, *Limnology and Oceanography Letters* **5**, 331 (2020).

[21] Y. Xie, Z. Sha, and M. Yu, Remote sensing imagery in vegetation mapping: a review, *Journal of plant ecology* **1**, 9 (2008).

[22] S. Majumder, K. Tamma, S. Ramaswamy, and V. Guttal, Inferring critical thresholds of ecosystem transitions from spatial data, *Ecology* **100**, e02722 (2019).

[23] W. Horsthemke and R. Lefever, Noise-induced transitions, *Noise in nonlinear dynamical systems* **2**, 179 (1989).

[24] J. Gradišek, S. Siegert, R. Friedrich, and I. Grabec, Analysis of time series from stochastic processes, *Physical Review E* **62**, 3146 (2000).

[25] R. Friedrich, J. Peinke, M. Sahimi, and M. R. R. Tabar, Approaching complexity by stochastic methods: From biological systems to turbulence, *Physics Reports* **506**, 87 (2011).

[26] R. Tabar, *Analysis and data-based reconstruction of complex nonlinear dynamical systems*, Vol. 730 (Springer, 2019).

[27] J. Jhawar and V. Guttal, Noise-induced effects in collective dynamics and inferring local interactions from data,

Philosophical Transactions of the Royal Society B **375**, 20190381 (2020).

[28] P. Rinn, P. G. Lind, M. Wächter, and J. Peinke, The Langevin Approach: An R Package for Modeling Markov Processes, *Journal of Open Research Software* **4**, 10.5334/jors.123 (2016).

[29] F. Dietrich, A. Makeev, G. Kevrekidis, N. Evangelou, T. Bertalan, S. Reich, and I. G. Kevrekidis, Learning effective stochastic differential equations from microscopic simulations: combining stochastic numerics and deep learning, *arXiv:2106.09004 [physics]* (2021), arXiv: 2106.09004.

[30] N. Evangelou, F. Dietrich, J. M. Bello-Rivas, A. Yeh, R. Stein, M. A. Bevan, and I. G. Kevrekidis, Learning Effective SDEs from Brownian Dynamics Simulations of Colloidal Particles, *arXiv:2205.00286 [cs, math]* (2022), arXiv: 2205.00286.

[31] S. L. Brunton, J. L. Proctor, and J. N. Kutz, Discovering governing equations from data by sparse identification of nonlinear dynamical systems, *Proceedings of the national academy of sciences* **113**, 3932 (2016).

[32] S. H. Rudy, S. L. Brunton, J. L. Proctor, and J. N. Kutz, Data-driven discovery of partial differential equations, *Science advances* **3**, e1602614 (2017).

[33] L. Boninsegna, F. Nüske, and C. Clementi, Sparse learning of stochastic dynamic equations, *The Journal of Chemical Physics* **148**, 241723 (2018), arXiv: 1712.02432.

[34] J. L. Callaham, J.-C. Loiseau, G. Rigas, and S. L. Brunton, Nonlinear stochastic modelling with langevin regression, *Proceedings of the Royal Society A* **477**, 20210092 (2021).

[35] Y. Huang, Y. Mabrouk, G. Gompper, and B. Sabass, Sparse inference and active learning of stochastic differential equations from data, *arXiv preprint arXiv:2203.11010* (2022).

[36] C. Gardiner, *Stochastic methods*, Vol. 4 (springer Berlin, 2009).

[37] A. Kolpas, J. Moehlis, and I. G. Kevrekidis, Coarse-grained analysis of stochasticity-induced switching between collective motion states, *Proceedings of the National Academy of Sciences* **104**, 5931 (2007).

[38] K. Lehnertz, L. Zabawa, and M. R. R. Tabar, Characterizing abrupt transitions in stochastic dynamics, *New Journal of Physics* **20**, 113043 (2018).

[39] Pydaddy tutorials – advanced function fitting, https://pydaddy.readthedocs.io/en/latest/tutorials/3/advanced_fitting.html (2022), [Online; accessed 1-May-2022].

[40] K. L. Drury, Shot noise perturbations and mean first passage times between stable states, *Theoretical Population Biology* **72**, 153 (2007).

[41] K. Johst and C. Wissel, Extinction risk in a temporally correlated fluctuating environment, *Theoretical Population Biology* **52**, 91 (1997).

[42] S. Shalev-Shwartz and S. Ben-David, *Understanding machine learning: From theory to algorithms* (Cambridge university press, 2014).

Supplementary Information for:
**PyDaddy: A Python package for discovering
stochastic dynamical equations from time series data**

Arshed Nabeel,^{1,*} Ashwin Karichannavar,^{1,†} Shuaib Palathingal,¹
Jitesh Jhawar,^{2,3} Danny Raj M.,⁴ and Vishwesha Guttal^{1,‡}

¹*Center for Ecological Sciences,
Indian Institute of Science, Bengaluru, India*

²*University of Konstanz, Konstanz, Germany*

³*Max Planck Institute of Animal Behaviour, Konstanz, Germany*

⁴*Department of Chemical Engineering,
Indian Institute of Science, Bengaluru, India*

S1. MATHEMATICAL DETAILS OF ESTIMATING DRIFT AND DIFFUSION

A. Discovering interpretable drift and diffusion functions

Consider a d -dimensional state variable \mathbf{x} , observed at some sampling interval Δt . Assuming that the time series was generated by an underlying SDE $\dot{\mathbf{x}} = \mathbf{f}(\mathbf{x}) + \mathbf{g}(\mathbf{x}) \cdot \boldsymbol{\eta}$, we define *instantaneous* drift and diffusion, as a function of t and the instantaneous value of the state variable \mathbf{x} , as:

$$\tilde{F}(t; \mathbf{x}) = \frac{\mathbf{x}(t + \Delta t) - \mathbf{x}(t)}{\Delta t} \quad (1)$$

$$\tilde{G}(t; \mathbf{x}) = \frac{(\mathbf{x}(t + \Delta t) - \mathbf{x}(t))(\mathbf{x}(t + \Delta t) - \mathbf{x}(t))^T}{\Delta t} \quad (2)$$

From these instantaneous drift and diffusion functions \tilde{F} and \tilde{G} , respectively, we find interpretable mathematical expressions for F and G following the approach of Brunton et. al. [?]. Briefly, we start with a *library* of candidate terms and use sparse regression to fit F or G as a linear combination of a small number of terms from the library.

Specifically, consider a *library* of candidate functions $\{F_1, F_2, \dots, F_k\}$. For instance, F_i could be monomials up to a specified degree, another suitable basis such as a Fourier or Chebyshev basis, or domain-specific basic functions tailored for the problem. We wish to represent the drift function F as a linear combination of only a few of these candidate functions. In other words, we would like to find coefficients ξ_i such that $F(x) = \sum_i \xi_i F_i(x)$ such that only a few of the ξ_i 's are nonzero. This can be achieved using sparse regression, as detailed in the next section.

Note that we use uppercase F and G to represent the estimated drift and diffusion to distinguish them from the actual \mathbf{f} and \mathbf{g} . The estimated F corresponds to \mathbf{f} , and G corresponds to $\mathbf{g}\mathbf{g}^T$.

B. Sparse regression framework for discovering drift and diffusion functions

Following [?], we pose the problem of discovering analytical expressions for drift and diffusion as a sparse regression problem. Here, discuss the details of the sparse regression procedure for the drift function, in the scalar case (the procedure for the diffusion function is identical).

Let $\mathbf{x}_{T \times 1}$ be a column vector containing the state variable x sampled at each point of time, i.e. $x_i = x(i\Delta t)$. T is the total number of observations. Let $\phi_{T \times 1}$ be a column vector containing the instantaneous drift values, i.e. $\phi_i = \tilde{F}(i\Delta t)$. We have a library of candidate functions $\{F_1, F_2, \dots, F_k\}$ for the drift function. Define a *dictionary matrix* $\Theta_{T \times k}$ with i th column given by $\Theta_i = F_i(\mathbf{x})$. The notation $F_i(\mathbf{x})$ is used as shorthand for evaluating F_i on each entry of \mathbf{x} . In terms of ϕ and Θ , the sparse regression problem corresponds to finding a sparse vector ξ that solves the equation

* Corresponding author; arshed@iisc.ac.in

† Equal contribution.

‡ Co-corresponding author; guttal@iisc.ac.in

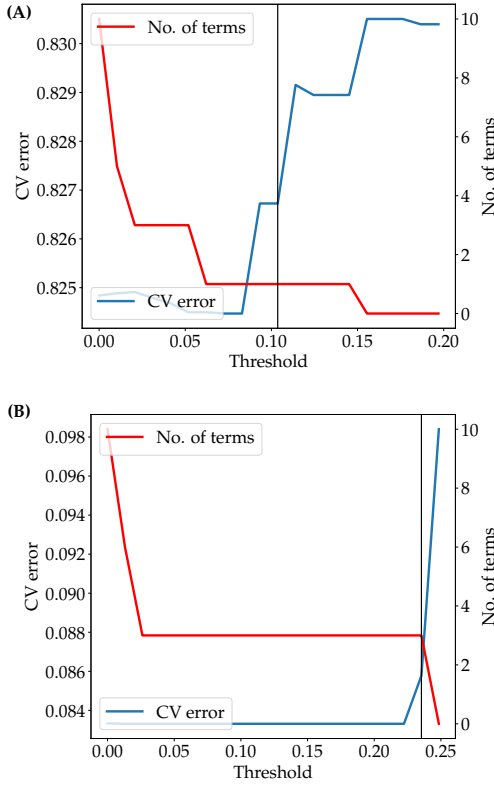


FIG. S1. **PyDaddy model selection.** When the `fit()` function is called with `tune=True`, PyDaddy uses cross validation to automatically choose the correct level of sparsification. (A) The cross-validation error and the number of selected terms at each level of sparsity, while fitting the drift function A_1 . The black line shows the threshold chosen by the cross validation algorithm, which produces a polynomial with just 1 term. (B) Similar plot for fitting the diffusion function B_{11} . The chosen threshold here corresponds to a polynomial with 3 terms.

$$\phi = \Theta \xi \quad (3)$$

To find a sparse solution for ξ , we use a procedure called *sequentially thresholded least squares* (STLSQ). The algorithm works as follows: first, a solution for ξ is found using ordinary least-squares. Now, all entries of ξ less than a pre-specified *sparsity threshold* are set to 0, and the corresponding columns are removed from the dictionary Θ . The procedure is now repeated with the remaining terms, until no more terms can be eliminated.

C. Model selection for sparse regression

The sparsity threshold in the STLSQ algorithm is an operational parameter that needs to be chosen appropriately to ensure that the right models are recovered. For different values of the sparsity threshold, we will get different models, and we need to use some criterion to choose the threshold that produces the best model. One approach is to use an appropriate information criterion, like Akaike Information Criterion (AIC): the model for which the information criterion is minimum is the one that achieves the best trade-off between model fit and model complexity.

An alternate approach, popular in the machine learning literature, is to choose the ideal model based on cross-validated accuracy [?]. We choose this approach, and use *k-fold cross validation* for model selection, which we briefly describe here.

The key idea behind cross-validation is to train a model using only part of the data, called *training set*, and evaluate the model performance on a *validation set*, different from the training set. A model that performs well on the validation set will not have overfit on the noise in the training data, and may be more generalisable. Specifically, the dataset is divided into k equal chunks. $k - 1$ of the chunks are used as the *training set* to fit the model, with the remaining chunk designated as the *validation set*. The error of the model on the validation set, called the *validation*

error, is now computed. The process is repeated with each of the k chunk designated as the validation set, and the average validation error is computed. The model that gives the minimum cross-validation error is chosen as the best model.

However, since model parsimony is crucial in our application, the model with the minimum cross validation error may not always be the best choice, as non-sparse models may sometimes end up getting selected. To avoid this, we instead sort the models in increasing order of complexity, and choose the model that achieves the *maximum drop* in cross-validation error from the previous model. Here, model complexity is defined simply as the number of terms with non-zero coefficients in the model. Fig. S1 shows the plot of cross validation error and model complexity (number of terms) for drift and diffusion for the fish schooling dataset. As the sparsification threshold is increased, the complexity of resulting model decreases. The chosen value of sparsification threshold is one beyond which the cross-validation error increases steeply.

D. Contrast to conventional approaches

Conventionally, the drift and diffusion as a function of \mathbf{x} are computed using the respective conditional moments. The drift (respectively, diffusion) at $\tilde{\mathbf{x}}$ can be approximated as

$$F(\tilde{\mathbf{x}}) = \left\langle \tilde{F}(t; \mathbf{x}) \right\rangle_{\mathbf{x}(t) \in [\mathbf{x}, \mathbf{x} + \epsilon]} \quad (4)$$

$$G(\tilde{\mathbf{x}}) = \left\langle \tilde{G}(t; \mathbf{x}) \right\rangle_{\mathbf{x}(t) \in [\mathbf{x}, \mathbf{x} + \epsilon]} \quad (5)$$

where the angular brackets indicate time averaged value of $\tilde{F}(t; \mathbf{x})$ (respectively, $\tilde{G}(t)$), computed for all time instances when \mathbf{x} is within a small bin of width ϵ around $\tilde{\mathbf{x}}$.

In this conventional approach, the accuracy of the estimated functions F and G depends on the sampling interval Δt . There is a bias-variance trade-off at play: smaller values of Δt gives estimates with smaller bias and higher variance, and vice versa. Therefore, subsampling the available time series with a larger Δt is sometimes required to get an optimal estimate ([?], SI Section S2 A).

A crucial point to note is that the bin-wise averaging step (Eq. 4, 5) is not required for the sparse regression: regression can be performed on the instantaneous drift and diffusion (Eq. 1, 2) directly. This eliminates the bin-width parameter ϵ from the estimation procedure. In addition, when using sparse regression, there is no need for subsampling the time series, as opposed to bin-wise averaging which requires an optimal choice of Δt (see SI Section S2 A).

We re-emphasize that our approach that combines sparse regression with the instantaneous drift and diffusion allowed us to eliminate two arbitrary parameter choices (namely, the bin width and the subsampling time scale) from the estimation procedure.

S2. ESTIMATION WITH LIMITED DATA

In this section, we examine the effects of data limitations on the estimation performance. Two aspects are considered, namely, the length of the time series, and the sampling interval.

A. Effect of time series length

In general, one would expect the estimation performance to increase when we have more data. For very short time series, the estimates are noisy and the estimation error is relatively high. As the amount of available data increases, the estimation error decreases.

Fig. S2 shows the average estimation error, with simulated data of different lengths (ranging from 10^4 to 10^6 time points), for different models. The averages are computed over 100 different instantiations of each model. As expected, the estimation error for drift decreases with increasing time series length. For diffusion, the estimates are fairly accurate even with short time series, and there is no significant decrease in the estimation error with longer time series.

For comparison, the estimation errors of the bin-wise averaging method are also shown. In general, the estimation errors with the bin-wise averages are much larger than PyDaddy estimation errors. This is due to the fact that the bin-wise approach estimates drift and diffusion functions independently for each bin, and disregards the overall

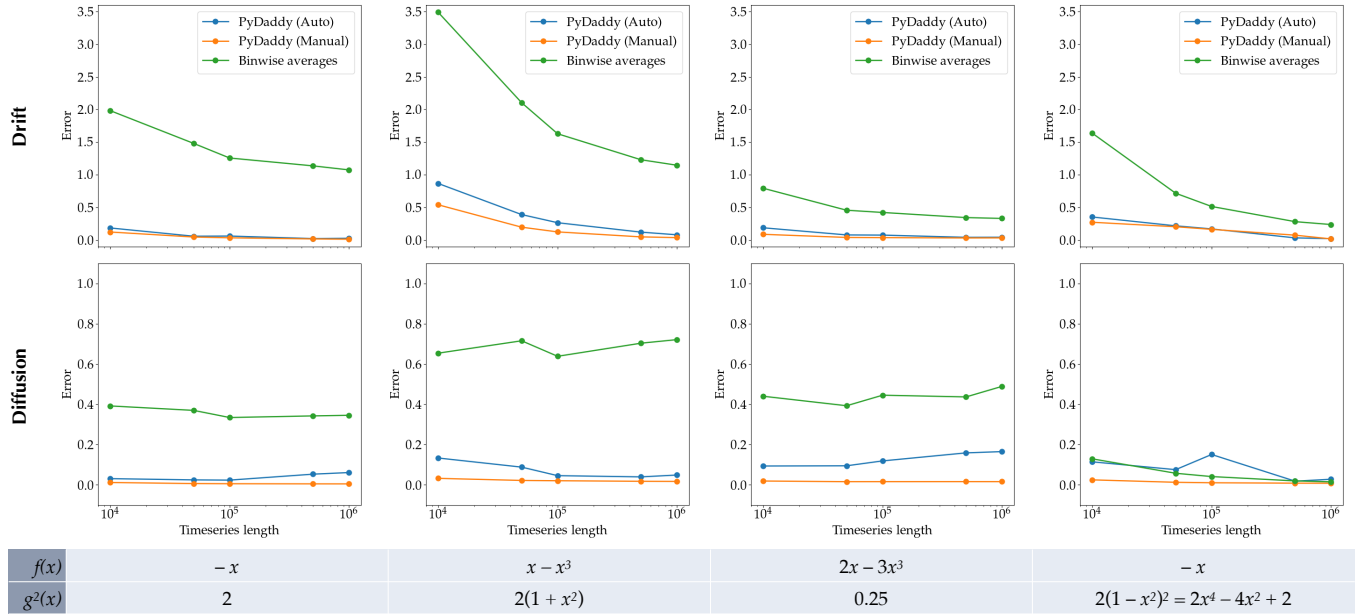


FIG. S2. **Effect of time series length on estimation error.** Estimation errors (relative r.m.s. error) for drift (top) and diffusion (bottom) for four example SDEs. The actual drift and diffusion functions are shown at the bottom. Estimation errors are plotted for conventional bin-wise estimation, PyDaddy estimation with automatic threshold tuning, and PyDaddy estimation with manual thresholds. In general, as the amount of available data (i.e. time series length) increases, estimation error of drift decreases. Estimation accuracy for diffusion is good even with shorter time series. For both drift and diffusion, PyDaddy achieves much better estimation accuracy than conventional bin-wise averaging, even for short time series.

shape and smoothness of the functions. Errors in estimates for individual bins therefore can become quite large when there are only a few samples in the bin. By fitting an analytic function to the jump moments, PyDaddy is able to capture the smoothness of the drift and diffusion functions to achieve better estimates.

B. Effect of sampling interval

In the conventional approach of estimating drift and diffusion functions as bin-wise averages, there is a bias-variance trade-off: as the sampling interval increases, the bias in the estimation of drift and diffusion increases, but the variance decreases. To obtain the best trade-off, one may need to subsample the time series at a Δt much larger than the resolution at which the data is available in [?]. Fig. S3 shows how, for the bin-wise estimates, the estimation error decreases to a minimum (due to decreasing variance) before starting to increase again as Δt increases. This is due to high variance in the bin-wise estimates for small values of Δt . The effect is particularly evident in the drift estimate.

However, this effect is absent in the sparse regression approach, and smaller Δt always yields smaller estimation errors. As described in SI Section S1 D, the smallest possible Δt (i.e., the temporal resolution at which the data is available in) is usually the best choice for estimation with PyDaddy, further subsampling only decreases estimation performance.

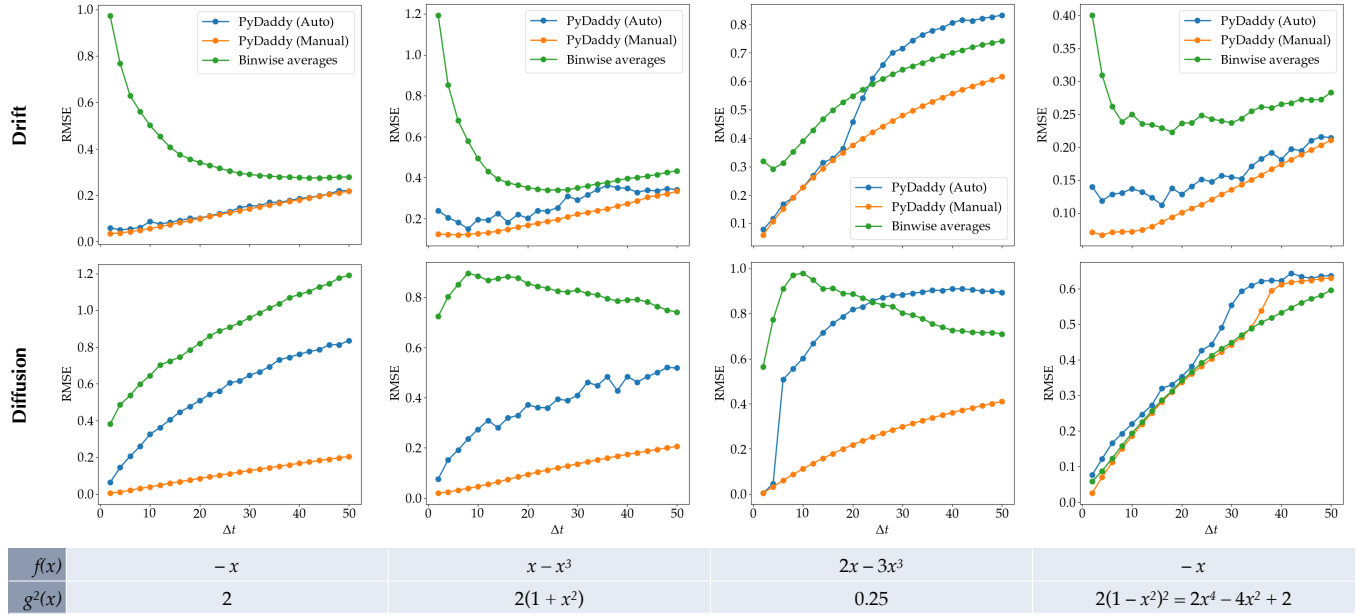


FIG. S3. **Effect of sampling time on estimation error.** Estimation errors (relative r.m.s. error) for drift (top) and diffusion (bottom), as a function of sampling interval Δt , for four example SDEs. The actual drift and diffusion functions are shown at the bottom. Estimation errors are plotted for conventional bin-wise estimation, PyDaddy estimation with automatic threshold tuning, and PyDaddy estimation with manual thresholds. For PyDaddy estimates, the estimation error always increases monotonically with subsampling time Δt . Contrast this with the bin-wise estimates, where the estimation error often has a non-monotonic trend.

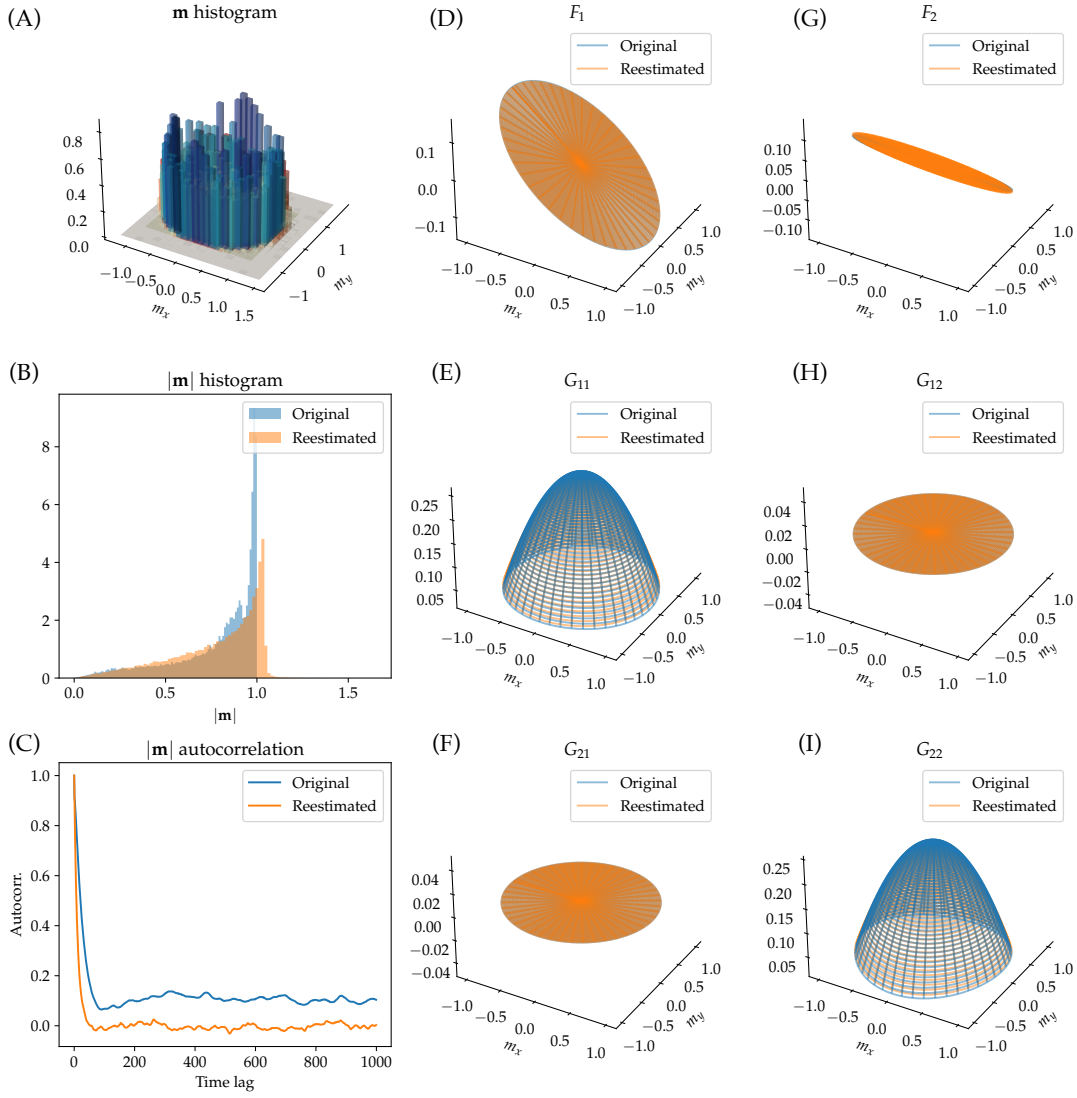


FIG. S4. Model diagnostics figure generated by PyDaddy. (A-B) Comparison of histograms of M and $|M|$ respectively, between the original time series and a time series simulated using the discovered SDE. (C) Autocorrelation functions of the simulated time series. (D-I) Comparison of the drift and diffusion functions between the original estimate and re-estimate (from the simulated data).